ELSEVIER

Journal of Organometallic Chemistry 635 (2001) 165–172

Journal of Organometallic Chemistry

www.elsevier.com/locate/jorganchem

A density functional study of the structures, vibrations and bond energies of dinitrogen phosphine complexes of the first transition series

Robert J. Deeth *

Inorganic Computational Chemistry Group, Department of Chemistry, University of Warwick, Coventry CV4 7AL, UK

Received 18 April 2001; accepted 15 June 2001

Abstract

The structures and vibrational properties of *trans*-$[V(N_2)_2(PH_3)_4]^-$, *trans*-$[Cr(N_2)_2(PH_3)_4]$, $[Mn(H)(N_2)(PH_3)_4]$, $[Fe(N_2)(PH_3)_4]$, $[Fe(H)(N_2)(PH_3)_4]^+$ and $[FeCl(N_2)(PH_3)_4]^+$ have been computed using density functional theory. Good reproduction of metal ligand bond lengths and the trend in N–N stretching frequencies ν(N–N) is obtained showing that simple PH_3 is a good model for the more complicated phosphine ligands employed experimentally. Analysis of the theoretical M–N binding energies shows a good correlation between increasing bond strength and decreasing ν(N–N). *trans*-$[V(N_2)_2(PH_3)_4]^-$ has the lowest value of ν(N–N) (~ 1740 cm^{-1}) and the largest calculated M–N_2 bond energy (223 kJ mol^{-1}) while $[Fe(H)(N_2)(PH_3)_4]^+$ has the highest value of ν(N–N) (~ 2100 cm^{-1}) and the lowest computed M–N_2 bond energy (126 kJ mol^{-1}). The biggest discrepancy between theory and experiment is for *trans*-$[V(N_2)_2(PH_3)_4]^-$. The error is removed by explicitly modelling solvation effects and the ion-pair interactions with alkali metals which are vital for stabilising dinitrogenvanadates(-1). The strong V–N_2 bond is apparently at odds with the reported lability of dinitrogenvanadate(-1) complexes. However, this assumes that the lability is reversible. The modelling suggests that N_2 loss is accompanied by decomposition.

Keywords: Dinitrogen complexes; Density functional theory; Electronic structures; Reactivity

1. Introduction

Dinitrogen is isoelectronic with carbon monoxide and the bonding in transition metal–N_2 complexes is thus expected to parallel the usual synergic σ-bonding/π-backbonding pattern. In many respects, dinitrogen complexes are similar to their carbonyl analogues although, given the more inert character of N_2, dinitrogen coordination chemistry is not as extensive [1].

A particular impetus for studying metal–N_2 species is biological nitrogen fixation. In contrast to the industrial Haber process (Eq. (1)) which requires high pressures and elevated temperatures, Nature converts N_2 to NH_3 at atmospheric pressure and ambient temperatures, albeit via a different stoichiometric process which, for conventional molybdenum-containing nitrogenase is given by Eq. (2) [2].

$$N_2 + 3H_2 \rightarrow 2NH_3 \quad (1)$$

$$N_2 + 8H^+ + 8e^- \rightarrow 2NH_3 + H_2 \quad (2)$$

The active site of the nitrogen fixing enzyme nitrogenase (N_2ase) contains a complicated cluster, FeMoco, (Fig. 1) containing both three- and four-coordinate iron centres joined via bridging sulphides to another metal, either Mo, V or Fe [3].

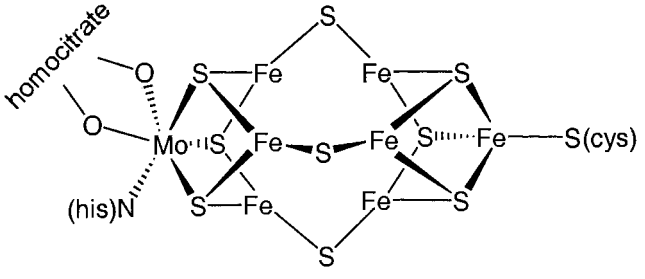

Fig. 1. Schematic representation of a proposed [2] FeMoco cofactor structure of molybdenum nitrogenase.

* Corresponding author. Tel.: +44-24-7652-3187; fax: +44-24-7652-4112.

E-mail address: r.j.deeth@warwick.ac.uk (R.J. Deeth).

0022-328X/01/$ - see front matter
PII: S0022-328X(01)01076-2

This cluster is believed to provide the N_2 binding site and effect its reduction to ammonia. The exact details are still being debated but the original idea that Mo is the initial site of N_2 binding, which was put forward prior to the 3-dimensional X-ray diffraction structural study of N_2ase itself, seems to have lost out in favour of the unusual three-coordinate iron sites [4] or even at one or more of the sulphur centres.

Many attempts have been made to develop functional models for N_2ase and some relatively simple dinitrogen complexes are indeed capable of converting at least some of the coordinated N_2 to NH_3 [1]. However, a reliable guide to those features which control N_2 binding and its activation towards protons is still lacking. The problem is complex and only limited success has been achieved in correlating experimental behaviour with the underlying molecular structures.

The approach in this laboratory [5,6] and elsewhere [4,7–11] has been to explore theoretical methods to study the fundamental nature of metal–dinitrogen binding to see whether a computational approach would provide a viable basis for designing new, more active compounds. Our first attempts were restricted to demonstrating that theory gave qualitatively correct trends when compared to experimental behaviour. These studies were limited by the computers and methods available at that time. Since then, the power of computational chemistry has increased enormously to the point where quantitative agreement between theory and experiment can be expected for a range of properties.

This paper revisits a series of complexes which are unusual in that they appear to run counter to the expectations of synergic σ-donation/π-back donation. Normally, a reduction in the frequency of the N–N stretching vibration from the isolated molecule value of 2331 cm^{-1} is associated with greater $M \rightarrow N_2$ π back-bonding and thus with greater $N \rightarrow M$ σ donation. However, complexes of the type $[V(N_2)_2(dmpe)_2]^-$ have very low N–N stretching frequencies, ν(N–N) ~ 1720–1760 cm^{-1} for dimethylphosphinoethane (dmpe) systems, yet are reported to be labile and to loose N_2 under reduced pressure [12], while other species such as $[Fe(N_2)H(dmpe)_2]^+$ have a high ν(N–N) of ~2100 cm^{-1} yet can be heated to decomposition without apparent loss of N_2 [13]. Based on qualitative extended Hückel molecular orbital (EHMO) theory, we found [5] that the M–N σ overlap and the N–N π overlap populations correlated with these experimental observations of 'anti-synergic' behaviour. Thus we argued that the electron rich V^{-1} centre discouraged σ donation but encouraged π back bonding while the electron poor Fe^{2+} centre encouraged σ donation and discouraged π back donation. These qualitative arguments can now be put to a quantitative test using modern density functional theory (DFT). These new results force us to rethink the bonding in these simple complexes.

2. Computational details

The DFT calculations were obtained using the Amsterdam Density Functional (ADF) programme suite version 2000.02 [14–17]. Geometries were optimised using both the local density approximation (LDA) and the Becke88/Perdew86 gradient corrected functional (BP86) [18,19]. Frequency calculations also considered the other gradient corrected functionals available in ADF namely Perdew–Wang [20] (PW91) and Lee–Yang–Parr [21] (LYP). The frozen-core approximation [22] was applied with orbitals 1s–2p frozen on the transition metals and phosphorus and the 1s orbital frozen for N and C. Basis sets comprised triple-ζ + polarisation STO expansions (basis IV), double-ζ + polarisation (basis III), double-ζ (basis II) or some combination of these as described in the text. Solvation energies were computed using the COSMO method implemented in ADF [23–25] with a dielectric constant of 32 and a probe radius of 2.0 Å.

3. Results and discussion

The original EHMO study was based on three simple dinitrogen complexes—*trans*-$[V(N_2)_2(dppe)_2]^-$, $[Fe(H)(N_2)(dmpe)_2]^+$ [13] and $[Fe(N_2)(depe)_2]$ [27] (dppe = diphenylphosphinoethane, depe = diethylphosphinoethane). In this work, three further structurally characterised systems are included. The neutral compounds *trans*-$[Cr(N_2)_2(dmpe)_2]$ [28,29] and $[Mn(N_2)(H)(dmpe)_2]$ [30] are isoelectronic with the anionic vanadium and cationic iron complexes, respectively. The chloro species $[FeCl(N_2)(depe)_2]^+$ [31] is included for further comparisons.

3.1. Geometries

A major shortcoming of EHMO theory is the lack of any automatic geometry optimisation. One is forced to rely on experimental structures rather than compute the structure from first principles. In contrast, accurate automatic geometry optimisation is routine with DFT and excellent agreement with experimental structural data can be anticipated. However, since the functionals commonly in use were not optimised explicitly for transition metal systems, it is always advisable to calibrate the choice of functional and basis set. Accordingly, we begin by optimising the structures of the six complexes (Table 1).

In common with previous work [35], we begin by replacing the bidentate phosphine ligands with two PH_3 molecules. The molecular symmetries have also been idealised to D_{2d} for the bis-dinitrogen species or C_{2v} for the mono-dinitrogen complexes as shown in Fig. 2.

Table 1
Observed and calculated bond lengths (Å)

Complex (method)	M–P	M–N	N–N	M–X
$[V(N_2)_2(dppe)_2]^-$ (exp [26])	2.42	1.92	1.13	–
$[V(N_2)_2(PH_3)_4]^-$ (LDA)	*2.29*	*1.98*	*1.14*	
$[V(N_2)_2(PH_3)_4]^-$ (BP86)	*2.34*	*1.94*	*1.15*	
$[Cr(N_2)_2(dmpe)_2]$ (exp [28,29])	2.30	1.87	1.12	–
$[Cr(N_2)_2(PH_3)_4]$ (BP86)	*2.30*	*1.88*	*1.14*	
$[Mn(H)(N_2)(dmpe)_2]$ (exp [30])	2.21	1.82	1.13	1.51
$[Mn(H)(N_2)(PH_3)_4]$ (BP86)	*2.22*	*1.84*	*1.14*	*1.58*
$[Fe(N_2)(depe)_2]$ (exp [32])	2.21 (ax) 2.19 (eq)	1.75	1.14	–
$[Fe(N_2)(PH_3)_4]$ (BP86)	*2.20* (ax) *2.18* (eq)	*1.81*	*1.14*	
$[Fe(H)(N_2)(hppd)]^+$ (exp [33]) [a]	2.22	1.87	1.07	1.53
$[Fe(H)(N_2)(dmpe)_2]^+$ (exp [13,34])	2.21	1.83	1.11	1.33
$[Fe(H)(N_2)(PH_3)_4]^+$ (BP86)	*2.23*	*1.85*	*1.12*	*1.51*
$[FeCl(N_2)(depe)_2]^+$ (exp [31])	2.29	1.78	1.09	2.31
$[FeCl(N_2)(PH_3)_4]^+$ (BP86)	*2.26, 2.27*	*1.80*	*1.12*	*2.32*

[a] hppd

= 1,1,4,7,10,10-Hexaphenyl-1,4,7,10-tetraphosphadecane-P,P′,P″,P‴.

The LDA-optimised bond lengths for *trans*-$[V(N_2)_2(PH_3)_4]^-$ give V–P distances 0.13 Å too short and V–N_2 distances 0.06 Å too long when compared to the dppe analogue. This result is intriguing given the normal expectation that the LDA leads to overbinding [36,37]. However, instead of both types of metal ligand bond being too short, the change in the V–P bond appears to be at the expense of the V–N_2 interaction which lengthens to compensate. These errors are significantly reduced with the BP86 gradient corrected functional which lengthens the V–P bond by 0.05 Å. This change is accompanied by a concomitant *shortening* of the V–N_2 bond by a similar amount. The final BP86 structure is in much better agreement with experiment although the computed V–P distance is still too short. We will return to this point later.

Given the superior performance of the BP86 functional, the structures of the remaining molecules were optimised at this level. The agreement between theory and experiment is excellent and suggests that for the present complexes, replacing the actual phosphine ligands with PH_3 is reasonable, at least so far as metal–ligand bond lengths are concerned.

3.2. Vibrational spectra

Given the usual connection between vibrational spectroscopy and the nature of the metal–dinitrogen bond, it is vital to demonstrate that DFT gives reliable vibrational frequencies. However, the ADF program estimates the second derivatives via finite differences of analytical first derivatives. For accuracy, each second derivative is estimated from two first derivatives which, for an N atom system, results in $6N + 1$ derivative calculations for a run using cartesian coordinates, i.e. one which also includes the (redundant) translations and rotations. Consequently, calculating the complete vibrational spectrum can be very time consuming and is in any case prone to numerical 'noise', especially for low-frequency motions.

High point-group symmetry reduces the number of unique degrees of freedom significantly. For example, a full (cartesian) frequency calculation for $[Cr(N_2)_2(PH_3)_4]$ requires 127 derivative evaluations which reduces to only 37 under D_{2d} symmetry. However, the high symmetry geometry does not usually correspond to a local minimum and several low-frequency imaginary modes result. These modes correspond to minor torsional motions of the PH_3 groups and are not a significant problem since we are only interested in the M–N and N–N stretching modes which have relatively high frequencies.

Table 2 compares the results from a full D_{2d} frequency calculation for $[Cr(N_2)_2(PH_3)_4]$ (column 1) with those from a partial calculation with only four degrees of freedom—the two Cr–N distances and the two N–N distances. Both N–N modes and the Cr–N sym-

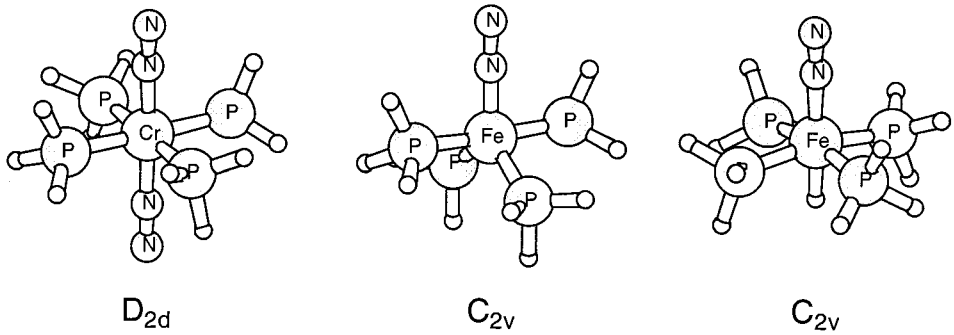

Fig. 2. Idealised symmetries showing orientation of phosphine H atoms.

Table 2
Sensitivity of computed vibrational frequencies to the number of degrees of freedom, functional and basis set for $[Cr(N_2)_2(PH_3)_2]$

Calc type	BP86/III Full	BP86/III Partial	LDA/III Partial	BP86/IV Partial	PW91/III Partial	BLYP/III Partial
ν_s(N–N)	2031	2030	2029	2026	2028	2021
ν_{as}(N–N)	2075	2075	2075	2070	2074	2066
ν_s(Cr–N_2)	403	404	396	407	408	410
ν_{as}(Cr–N_2)	487	514	499	511	517	524

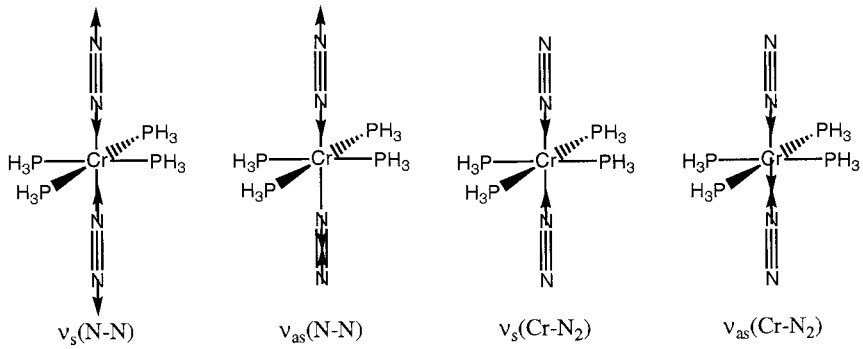

Fig. 3. Schematic representation of the N–N and Cr–N_2 stretching vibrations.

metric stretch are insensitive to basis set, functional and the number of degrees of freedom. Only the Cr–N asymmetric stretch changes significantly. Animation of all four vibrations from the full calculation (Fig. 3) shows that this mode is special in that the metal atom moves out of the equatorial plane and so there is a contribution from the Cr–P bonds and the N–Cr–P angles which is not accounted for in the partial frequency calculation.

In the IR spectrum, the active N–N stretching mode is usually more easy to locate than the M–N modes. Table 3 presents a comparison of all the computed N–N mode frequencies and intensities (BP86, full cartesian calculation) with the available experimental data while Fig. 4 shows the same comparison except that where more than one experimental datum exists, the average has been used. Although the calculated data are systematically higher than experiment by around 100 cm^{-1} ($\sim 5\%$), the qualitative trends are remarkably similar.

Theory appears to perform rather worse for $[V(N_2)_2(PH_3)_4]^-$, overestimating the frequency by more than 200 cm^{-1}. This is *not* due to the use of simple PH_3 ligands. A full BP86 geometry optimisation followed by a partial frequency calculation for the complete $[V(N_2)_2(dmpe)_2]^-$ system does not significantly alter the metal–ligand distances and only lowers the estimated N–N mode frequency by 28 to 1913 cm^{-1} (Table 4). In any event, the calculated trend is satisfactory suggesting that just as for the structures, the calculated vibrational frequencies for simplified PH_3 species are reasonable approximations for compounds with more complicated phosphine ligands.

3.3. Binding energies

A powerful feature of the ADF package is the ability to analyse the total binding energies in terms of frag-

Table 3
Comparison of calculated and observed N–N stretching mode frequencies (IR active band in bold)

Complex (Symmetry)	ν(N–N): Calc	Intensity (km mol^{-1}) (calc)	ν(N–N): Obs
$[V(N_2)_2(PH_3)_4]^-$	1941	2120	1721 [a], 1758 [b]
(D_{2d})	1976	0	
$[Cr(N_2)_2(PH_3)_4]$	2031	1532	1932 [d]
(D_{2d})	2075	0	
$[Mn(H)(N_2)(PH_3)_4]$ (C_{2v})	2075	690	–
$[Fe(N_2)(PH_3)_4]$ (C_{2v})	2075	737	1955 [c]
$[Fe(H)(N_2)(PH_3)_4]$ (C_{2v})	2185	351	2090 [c], 2106 [d]
$[FeCl(N_2)(PH_3)_4]$ (C_{2v})	2165	328	2088 [c]

[a] *trans*-$Na_2[V(N_2)_2(dmpe)_2]$.
[b] *trans*-$Li[V(N_2)_2(dmpe)_2]$.
[c] depe complex.
[d] dmpe complex.

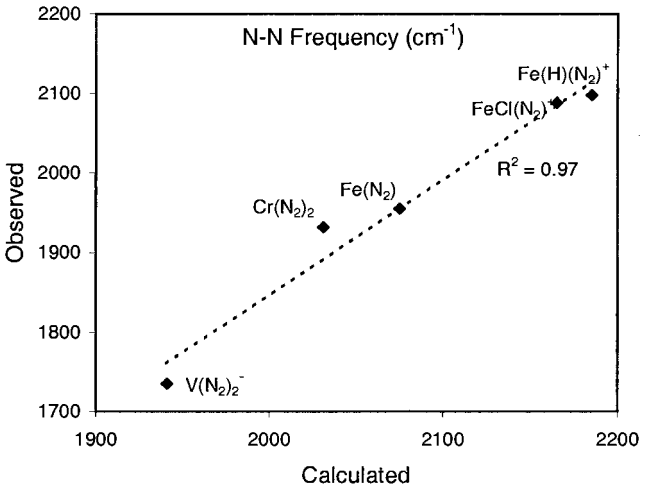

Fig. 4. Comparison of calculated and observed (averaged) N–N stretching mode frequencies.

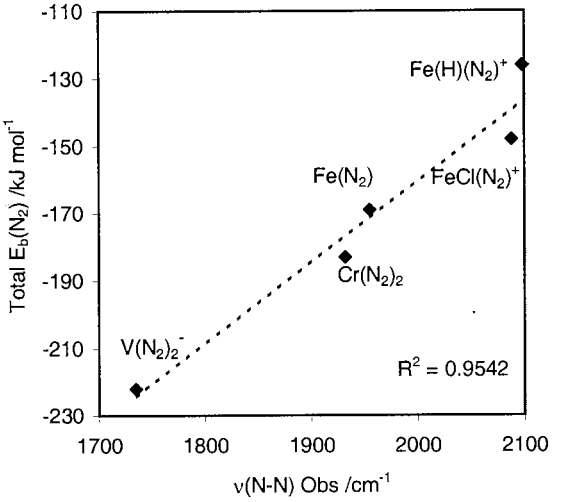

Fig. 5. Comparison of observed IR stretching frequencies, ν(N–N) (cm^{-1}) and calculated metal–N_2 binding energy, $E_b(N_2)$ (kJ mol^{-1}).

Table 4
Calculated (BP86) structural and N–N stretching frequencies for $[V(N_2)_2(dmpe)_2]^-$

V–P	2.34 Å
V–N	1.93 Å
N–N	1.15 Å
ν_s(N–N)	1958 cm^{-1} (0.05 km mol^{-1})
ν_{as}(N–N)	1913 cm^{-1} (1819 km mol^{-1})

ments [38]. Here, each complex is divided into N_2 fragments and a metal phosphine fragment (the latter includes the H or Cl ligand as appropriate) and the interactions between these pieces calculated.

The overall binding energy per M–N_2 bond, $E_b(N_2)$, is divided into two main parts. The first so-called 'steric' part models the energy associated with bringing the various fragments from infinite separation up to their bonded configuration but without allowing the charge clouds to overlap. This term is expected to be positive. The second term models the effects of allowing the charge clouds to interact. This 'orbital' term thus monitors the bonding between fragments and is expected to be negative. Moreover, the orbital interactions can be separated by irreducible representation. In the present set of molecules, this provides a more or less clean division between M–N_2 σ interactions (of a_1 symmetry) and M–N_2 π interactions (of e symmetry in D_{2d} or the sum of b_1 and b_2 symmetries in C_{2v}).

The calculated energies are collected in Table 5. Aspects of these data are displayed in Figs. 5 and 6.

First, consider the total binding energy per N_2 ligand (Fig. 5). There is a good correlation between the calculated M–N_2 bond strength, $E_b(N_2)$, and the magnitude of the measured N–N stretching frequency, ν(N–N). As shown in Fig. 6, this correlates with the M–N π orbital interaction rather than any σ binding. That is, the more M → N π back bonding, the greater is the reduction in ν(N–N). All of this is as we stated before [5]. However, the quantitative DFT calculations show that our previous assertion that the M–N bond strength would be dominated by σ interactions alone is clearly unfounded. DFT predicts that this series of molecules should behave as expected based on the synergic bonding model.

The π/σ ratio in the M–N_2 bonds correlates with the formal charge on the metal. For the V^{-1} complex, the value is ~3.5 which reduces to 2.3–1.7 for the neutral metal centres (Cr, Mn and Fe) and then drops to 1.4–1.2 for the formally Fe^{2+} complexes. Thus, the

Table 5
M–N_2 bond energy decomposition analysis

Complex	$[V(N_2)_2(PH_3)_4]^-$	$[Cr(N_2)_2(PH_3)_4]$	$[Mn(H)(N_2)(PH_3)_4]$	$[Fe(N_2)(PH_3)_4]$	$[Fe(H)(N_2)(PH_3)_4]^+$	$[FeCl(N_2)(PH_3)_4]^+$
Steric	138	159	161	189	142	172
Orb: a_1	−77	−97	−111	−134	−114	−144
Orb b_1/e	−266	−225	−116	−136	−78	−89
b_2			−111	−88	−76	−87
Total Orb	−360	−342	−338	−358	−268	−320
π/σ	3.5	2.3	2.0	1.7	1.4	1.2
Total per N_2	−223	−183	−177	−168	−126	−148

All energy values in kJ mol^{-1}.

more electron rich the metal, the greater the proportion of M–N π back-bonding. The trend extends to a more detailed level in that the π/σ ratio drops from $[Cr(N_2)_2(PH_3)_4]$ to $[Mn(H)(N_2)(PH_3)_4]$ to $[Fe(N_2)(PH_3)_4]$ which correlates with the general increase in metal electronegativity on crossing the series from left to right while the ratio for $[FeCl(N_2)(PH_3)_4]^+$ is smaller than that for $[FeH(N_2)(PH_3)_4]^+$ consistent with the more electronegative Cl ligand making the Fe centre even more electron poor.

3.4. Lability of coordinated N_2

The DFT calculations on model phosphine species give an excellent account of the physical structural and vibrational data and yet this success does not appear to extend to predicting reactivity. The problem is that theory predicts that the V complex has the strongest metal–dinitrogen interaction and yet Rehder has reported extensive data on dinitrogenvanadates(-1) which are 'labile' and, under reduced pressure, lose N_2 [12]. These complexes are even more unusual in that there is evidence of 'close contact ion-pair interaction' and are stable and isolable only in the presence of Li^+ and Na^+ countercations. Thus, both the IR data and theory agree on a strong V–N_2 bond yet the ligand apparently falls off quite easily. The challenge to theory therefore is to attempt to rationalise these apparently conflicting observations.

Carbon monoxide is reported [12] to replace N_2 in $M[V(N_2)_2(dmpe)_2]$. To test that DFT does not have some pathological problem with vanadium–phosphine compounds, the V–CO binding energies for *trans*-$[V(CO)_2(PH_3)_4]^-$ were computed in an identical way to the analogous N_2 compound. Consistent with experiment, the calculated V–CO binding energy per CO is -298 kJ mol^{-1}, 75 kJ mol^{-1} stronger than the V–N_2 bond in the analogous dinitrogen species.

The data in Table 3 show that theory consistently overestimates the N–N stretching frequency, with $[V(N_2)_2(PH_3)_4]^-$ being the worst case. The computations on $[Cr(N_2)_2(dmpe)_2]$ show this is not due to the use of PH_3 as a model ligand so two further types of calculation were carried out to probe the sources of this error.

First, explicit alkali metal cations were added to simulate the reported formation of ion pairs. Based on the crystal structure of $[Na(thf)][V(N_2)_2(dppe)_2]$ [26], two M^+ cations were placed on the V–N axis, one for each N_2 so as to maintain the overall D_{2d} symmetry. Selected calculated structural and spectroscopic data are given in Table 6.

The calculated M–L distances for the $\{M_2[V(N_2)_2(PH_3)_4]\}^+$ systems show a 0.04–0.05 Å lengthening of the V–P distance and a similar shortening of the V–N_2 bond length relative to the isolated anionic complex. The former change improves the agreement with the reported V–P distance of 2.43 Å in $[Na(thf)][V(N_2)_2(dppe)_2]$ while the second change leads to an underestimate by about the same amount (~ 0.02 Å) as the previous calculations overestimated the V–N_2 contact. The calculated N···Na distance of 2.24 Å is about 0.2 Å shorter than in the experimental crystal structure.

The structural changes in the complex are accompanied by a reduction of up to 92 cm^{-1} in the calculated IR active N–N stretching mode frequency. That is, about half the original discrepancy between theory and experiment is recovered. The vibrational frequency decreases in the sequence $K^+ > Na^+ > Li^+$ which is paralleled by a reduction in the cations' Mulliken charges from 0.94 for K^+ to 0.82 for Na^+ to 0.74 for Li^+. That is, by $\{Li_2[V(N_2)_2(PH_3)_4]\}^+$, half of the -1 charge on the complex has been displaced onto the countercations. Although the model is relatively crude, these data show an increasingly important effect as the size of the

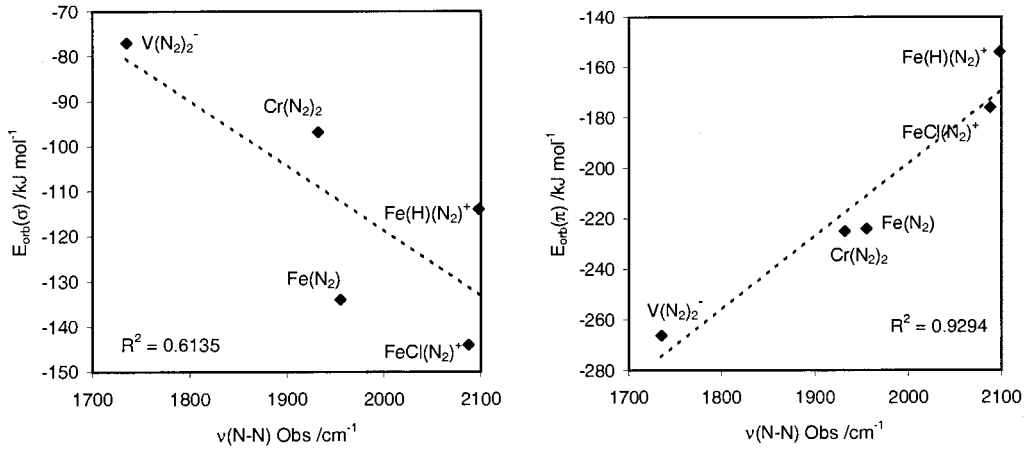

Fig. 6. Comparison of observed IR stretching frequencies, ν(N–N) (cm^{-1}) with the calculated orbital contributions to the M–N_2 σ and π binding energies, $E_{orb}(\sigma)$ and $E_{orb}(\pi)$ (kJ mol^{-1}).

Table 6
Calculated structural and vibrational data for $\{M_2[V(N_2)_2(PH_3)_4]\}^+$ complexes, M = Li^+, Na^+ and K^+

M	V–P (Å)	V–N (Å)	N–N (Å)	N···M	ν(N–N) [a] (cm^{-1})
Li	2.39	1.88	1.17	1.86	1849 (4090) 1934 (0)
Na	2.38	1.89	1.17	2.24	1859 (3962) 1936 (0)
K	2.37	1.89	1.16	3.73	1869 (3741) 1940 (0)

[a] Intensities in km mol^{-1} in parentheses.

alkali metal cation decreases which is consistent with the observation that only Li^+ and Na^+ exert sufficient influence to form stable complexes.

The second type of calculation attempts to account for solvation effects. So far, all the modelling has been carried out in vacuo which, judging by the good agreement with experimental parameters, appears to be justified. However, the vanadium(−1)–dinitrogen compounds are sensitive to the solvent; for example, attempts to precipitate bis(dinitrogen) complexes with pentane or hexane yield 'black, pyrophoric powders' [12]. Within the ADF package, solvation effects may be modelled using the COSMO method which treats the solvent as a polarisable continuum [23–25,39]. Geometry optimisation of $[V(N_2)_2(PH_3)_4]^-$ yields V–P and V–N distances of 2.43 and 1.90 Å, respectively, in near perfect agreement with the comparable bond lengths in $[Na(thf)][V(N_2)_2(dppe)_2]$. The N–N distance has also lengthened slightly to 1.17 Å which is consistent with the new N–N stretching frequency of 1683 cm^{-1}. However, this new value is now 40–70 cm^{-1} *lower* than experiment. Comparable COSMO calculations for *trans*-$[Cr(N_2)_2(PH_3)_4]$ show similar structural changes (Cr–P lengthens by 0.08 Å, Cr–N_2 shortens by 0.02 Å and N–N lengthens by 0.02 Å) and a 200 cm^{-1} reduction in ν(N–N) such that the new value is about 100 cm^{-1} lower than experiment. Thus, the COSMO corrections have the correct sense but are somewhat too large.

Overall, the calculated structural and spectroscopic properties of $[V(N_2)_2(PH_3)_4]^-$ are thus in good agreement with experiment yet we are still faced with the issue that these complexes are labile but have the largest computed metal–N_2 binding energy. Of course, the V–N bond energy is strengthened at the expense of a weakening N–N bond. However, calculations for free N_2 with bond lengths of 1.13 and 1.17 Å show an increase in the total energy of only about 20 kJ mol^{-1} compared to an (in vacuo) estimated 445 kJ mol^{-1} *decrease* in binding energy between $[V(PH_3)_4]^-$ and two N_2 fragments. Solvation effects in the modelling will not be large enough to counter the strong tendency for the formation of V–N bonds. For these systems, simple extrapolations based on the calculated properties of the ground state do not give the correct description of their reactivities.

4. Conclusions

DFT is an excellent computational method for probing the structure and vibrational properties of first row transition metal dinitrogen complexes. For the species *trans*-$[V(N_2)_2(PH_3)_4]^-$, *trans*-$[Cr(N_2)_2(PH_3)_4]$, $[Mn(H)(N_2)(PH_3)_4]$, $[Fe(N_2)(PH_3)_4]$ and $[Fe(H)(N_2)(PH_3)_4]^+$, good reproduction of metal ligand bond lengths and the trend in N–N stretching frequencies ν(N–N) is obtained. In these properties, simple PH_3 is a good model for the more complicated phosphine ligands employed experimentally.

Analysis of the theoretical M–N binding energies shows a good correlation between increasing bond strength and decreasing ν(N–N). Hence, in contrast to our previous conclusions based on qualitative EHMO theory, these complexes are completely 'normal' with respect to the predictions of the synergic bonding model. Thus, *trans*-$[V(N_2)_2(PH_3)_4]^-$ has the lowest value of ν(N–N) and the largest calculated M–N_2 bond energy while $[Fe(H)(N_2)(PH_3)_4]^+$ has the highest value of ν(N–N) and the lowest computed M–N_2 bond energy. Moreover, the π/σ ratio of the M–N bond correlates with the formal metal charge. Thus, the electron rich V^{-1} centre encourages back bonding and has the highest π/σ ratio of $\sim$3.5 while the relatively electron poor Fe^{2+} centres have lowest ratios of $\sim$1.2–1.4.

The strong V–N_2 bond is at odds with the reported lability of dinitrogenvanadate(−1) complexes [12]. However, this statement implies that the lability is reversible. If this were the case then the DFT should have been able to capture it by, for example, demonstrating that the energy of the complex is higher than the isolated fragments. Either the DFT is failing somehow or the 'lability' relates to a more complex process than simple N_2 detachment. In the absence of an explicit statement that N_2 loss under reduced pressure is, in fact, reversible, the modelling suggests that N_2 loss is accompanied by decomposition of some sort. If so, then unless the identities of the decomposition products are

know, it is not possible to demonstrate the 'lability' theoretically. Given the reported sensitivity of these complexes to the presence of small alkali metal cations and to the nature of the solvent, the possibilities are numerous. Thus, while theory gives an excellent description of the physical properties of these complexes, it is struggling to explain their chemical stability and reactivity.

Acknowledgements

The author acknowledges the support of the EPSRC Joint Research Equipment Initiative for the provision of computer equipment.

References

[1] M.D. Fryzuk, S.A. Johnson, Coord. Chem. Rev. 200 (2000) 379–409.
[2] W. Kaim, B. Schwederski, Bioinorganic Chemistry: Inorganic Elements in the Chemistry of Life, Wiley, Chichester, 1994.
[3] E.I. Stiefel, ACS Symp. Series 535 (1993) 1–19.
[4] I.G. Dance, Aust. J. Chem. 47 (1994) 979–990.
[5] R.J. Deeth, S.A. Langford, J. Chem. Soc. Dalton Trans. (1995) 1–4.
[6] R.J. Deeth, C.N. Field, J. Chem. Soc. Dalton Trans. (1994) 1943–1948.
[7] A.J. Bridgeman, O.M. Wilkin, N.A. Young, Inorg. Chem. Commun. 3 (2000) 681–684.
[8] V.M.E. Bates, G.K.B. Clentsmith, F.G.N. Cloke, J.C. Green, H.D.L. Jenkin, Chem. Commun. (2000) 927–928.
[9] N. Lehnert, F. Tuczek, Inorg. Chem. 38 (1999) 1659–1670.
[10] N. Lehnert, F. Tuczek, Inorg. Chem. 38 (1999) 1671–1682.
[11] P. Roussel, P. Scott, J. Am. Chem. Soc. 120 (1998) 1070–1071.
[12] H. Gailus, C. Woitha, D. Rehder, J. Chem. Soc. Dalton Trans. (1994) 3471–3477.
[13] A. Hills, D.L. Hughes, M. Jimenez-Tenorio, G.J. Leigh, A.T. Rowley, J. Chem. Soc. Dalton Trans. (1993) 3041.
[14] E.J. Baerends, A. Bérces, C. Bo, P.M. Boerrigter, L. Cavallo, L. Deng, R.M. Dickson, D.E. Ellis, L. Fan, T.H. Fischer, C. Fonseca Guerra, S.J.A. van Gisbergen, J.A. Groeneveld, O.V. Gritsenko, F.E. Harris, P. van den Hoek, H. Jacobsen, G. van Kessel, F. Kootstra, E. van Lenthe, V.P. Osinga, P.H.T. Philipsen, D. Post, C.C. Pye, W. Ravenek, P. Ros, P.R.T. Schipper, G. Schreckenbach, J.G. Snijders, M. Sola, D. Swerhone, G. te Velde, P. Vernooijs, L. Versluis, O. Visser, E. van Wezenbeek, G. Wiesenekker, S.K. Wolff, T.K. Woo, T. Ziegler, ADF 2000.01; Scientific Computing and Modelling NV, Free University, Amsterdam, 2000.
[15] E.J. Baerends, D.E. Ellis, P. Ros, Chem. Phys. 2 (1973) 41.
[16] L. Versluis, T.J. Ziegler, Chem. Phys. 88 (1988) 322–328.
[17] C. Fonseca Guerra, J.G. Snijders, G. te Velde, E.J. Baerends, Theor. Chem. Acc. 99 (1998) 391.
[18] A.D. Becke, Phys. Rev. A 38 (1988) 3098–3100.
[19] J.P. Perdew, Phys. Rev. B Condensed Matter 33 (1986) 8822–8824.
[20] J.P. Perdew, J.A. Chevary, S.H. Vosko, K.A. Jackson, M.R. Pederson, D.J. Singh, C. Fiolhais, Phys. Rev. B 46 (1992) 6671.
[21] C.T. Lee, W.T. Yang, R.G. Parr, Phys. Rev. B Condensed Matter 37 (1988) 785–789.
[22] E.J. Baerends, D.E. Ellis, P. Ros, Theoret. Chim. Acta 27 (1972) 339.
[23] A. Klamt, G. Schüürmann, J. Chem. Soc. Perkin Trans. 2 (1993) 799.
[24] A.J. Klamt, Phys. Chem. 99 (1995) 2224.
[25] A. Klamt, V.J. Jones, Chem. Phys. 105 (1996) 9972.
[26] D. Rehder, C. Woitha, W. Priebsch, H. Gailus, Chem. Commun. (1992) 364.
[27] S. Komiya, M. Akita, A. Yoza, N. Kasuga, V. Fukuoka, Y. Kai, Chem. Commun. (1993) 787.
[28] G.S. Girolami, J.E. Salt, G. Wilkinson, M. Thornton-Pett, M.B. Hursthouse, J. Am. Chem. Soc. 105 (1983) 5954.
[29] J.E. Salt, G.S. Girolami, G. Wilkinson, M. Motevalli, M. Thornton-Pett, M.B. Hursthouse, J. Chem. Soc. Dalton Trans. (1985) 685.
[30] C. Perthuisot, M. Fan, W.D. Jones, Organometallics 11 (1992) 3622.
[31] B.E. Wiesler, N. Lehnert, F. Tuczek, J. Neuhausen, W. Tremel, Angew. Chem. Int. Ed. Engl. 37 (1998) 815.
[32] C. Perthuisot, W.D. Jones, New J. Chem. (Nouv. J. Chim.) 18 (1994) 621.
[33] C.A. Ghilardi, S. Midollini, L. Sacconi, P. Stoppioni, J. Organomet. Chem. 205 (1981) 193.
[34] I.E. Buys, L.D. Field, T.W. Hambley, A.E.D. McQueen, Acta Crystallogr. Sect. C (Cr. Str. Comm.) 49 (1993) 1056.
[35] R.J. Deeth, J. Chem. Soc. Dalton Trans. (1993) 3711–3713.
[36] M.R. Bray, R.J. Deeth, V.J. Paget, P.D. Sheen, Int. J. Quant. Chem. 61 (1997) 85–91.
[37] T. Ziegler, Chem. Rev. 91 (1991) 651–667.
[38] T. Ziegler, A. Rauk, Inorg. Chem. 18 (1979) 1558.
[39] C.C. Pye, T. Ziegler, Theor. Chem. Acc. 101 (1999) 396.